ELSEVIER

Palaeogeography, Palaeoclimatology, Palaeoecology 176 (2001) 177–192

PALAEO

www.elsevier.com/locate/palaeo

Reconstruction of paleohydrology and paleohumidity from oxygen isotope records in the Bolivian Andes

Brent B. Wolfe[a,*], Ramon Aravena[a], Mark B. Abbott[b,1], Geoffrey O. Seltzer[c], John J. Gibson[d,2]

[a] *Department of Earth Sciences, University of Waterloo, Waterloo, ON, Canada N2L 3G1*
[b] *Department of Geosciences, Morrill Science Center, P.O. Box 35820, University of Massachusetts, Amherst, MA 01003-5820, USA*
[c] *Heroy Geology Laboratory, Department of Earth Sciences, Syracuse University, Syracuse, NY 13244-1070, USA*
[d] *Department of Geography, University of Waterloo, Waterloo, ON, Canada N2L 3G1*

Received 6 September 2000; received in revised form 9 July 2001; accepted 18 July 2001

Abstract

Cellulose-inferred lake water $\delta^{18}O$ ($\delta^{18}O_{lw}$) records from Lago Potosi (LP), a seasonally closed lake in a watershed that is not currently glaciated, and Lago Taypi Chaka Kkota (LTCK) [previously reported in Abbott et al., 2000. Quat. Sci. Rev. 19, 1801–1820], an overflowing lake in a glaciated watershed, provide the basis for late Pleistocene and Holocene paleoclimatic reconstruction in the Bolivian Andes. Deconvolution of the histories of changing evaporative isotopic enrichment from source water $\delta^{18}O$ in the lake sediment records is constrained by comparison to the Sajama ice core oxygen isotope profile, whereas local hydrological influence is distinguished from the regional moisture balance history by the response of the different catchments to climate change. Overall, variations in the LP $\delta^{18}O_{lw}$ record appear to be dominantly controlled by evaporative ^{18}O-enrichment, reflecting shifts in local effective moisture. This record is used to generate a preliminary quantitative reconstruction of summer relative humidity spanning the past 11 500 cal yr on the basis of an isotope-mass balance model. Results indicate that the late Pleistocene was moist with summer relative humidity values estimated at 10–20% greater than present. Increasing aridity developed in the early Holocene with maximum prolonged dryness spanning 7500–6000 cal yr BP at LP, an interval characterized by summer relative humidity values that may have been 20% lower than present. Highly variable but dominantly arid conditions persist in the mid- to late Holocene, with average summer relative humidity values estimated at 15% below present, which then increase to about 10–20% greater than present by 2000 cal yr BP. Slightly more arid conditions characterize the last millennium with summer relative humidity values ranging from 5–10% lower than present. Similar long-term variations are evident in the LTCK $\delta^{18}O_{lw}$ profile, except during the early Holocene when lake water evaporative ^{18}O-enrichment in response to low relative humidity appears to have been offset by enhanced inflow from ^{18}O-depleted snowmelt or groundwater from the large catchment. Although some temporal offset is evident, significant correspondence occurs between the isotope-inferred paleohumidity reconstruction and other paleohydrological proxies from the region. These

[1] Present adress: Department of Geology and Planetary Science, University of Pittsburgh, Pittsburgh, PA 15260-3332, USA.
[2] Present adress: Isotope Hydrology Section, International Atomic Energy Agency, Wagramer Strasse 5, P.O. Box 100, A-1400 Vienna, Austria.
* Corresponding author. Fax: +1-519-746-0183. *E-mail address:* bwolfe@sciborg.uwaterloo.ca (B.B. Wolfe).

PII: S0031-0182(01)00337-6

results support the contention that millennial-scale variations in tropical moisture balance may be linked to changes in summer insolation.

Keywords: Bolivian Andes; oxygen isotopes; cellulose; paleohydrology; paleohumidity; late Pleistocene; Holocene

1. Introduction

Large moisture fluctuations are dominant features of late Pleistocene and Holocene climate on the Bolivian Altiplano. Wetter conditions compared to the present characterized the late Pleistocene and early Holocene as indicated by pluvial lake high stands spanning from prior to 19 000 to about 14 000 and 10 700 to 9500 cal yr BP[3] (Clayton and Clapperton, 1997; Sylvestre et al., 1999). Marked aridity, however, is believed to have prevailed during most of the Holocene from about 9500 to 3900 cal yr BP, based mainly on studies of sediment cores from Lake Titicaca (Wirrmann and de Oliviera Almeida, 1987; Wirrmann and Mourguiart, 1995; Mourguiart et al., 1998; Cross et al., 2000; Baker et al., 2001) and seismic-reflection profiles of the basin (Seltzer et al., 1998). New paleo-water level estimates suggest that Lake Titicaca experienced lowest lake levels between 8000 and 5500 cal yr BP (Baker et al., 2001). Desiccation may have been widespread at this time in the shallower southern basin of Lake Titicaca and likely in many other ephemeral lakes resulting in discontinuous sedimentary records, which has hampered Holocene paleoclimatic reconstruction in this region. Increasingly moist conditions at about 3500 cal yr BP are suggested by the rise in Lake Titicaca to the overflow level, although highly variable moisture conditions define the late Holocene based on reconstructed 15–25-m water level fluctuations including several pronounced drought events (Abbott et al., 1997a). Linkages have been proposed between these climatic variations during the late Holocene and the history of ancient civilizations (Binford et al., 1997).

Multi-proxy studies of Lago Taypi Chaka Kkota (LTCK), presently an overflowing lake in a glaciated watershed of the Cordillera Réal of Bolivia 20 km from Lake Titicaca, provide one of the few largely continuous Holocene lake records of paleohydrological change in this region (Abbott et al., 1997b, 2000). During the mid- to late Holocene, the oxygen isotope composition of the lake water inferred from analysis of lake sediment cellulose averaged 6‰ higher than present due to greater evaporative ^{18}O-enrichment. This is comparable to lakes in non-glaciated watersheds in the region today, which drop below the overflow level during the dry season. Significant aridity during the mid-Holocene was also suggested by prevalence of shallow-water non-glacial periphytic diatom taxa as well as enrichment of ^{13}C and ^{15}N in bulk organic matter possibly attributable to loss of labile fractions due to periodic desiccation. Wetter conditions are suggested after 2300 cal yr BP by a decline in lake water $^{18}O/^{16}O$ and return of diatom assemblages characteristic of a proglacial setting.

The centennial-scale paleoclimate record derived from LTCK is broadly consistent with that from Lake Titicaca, indicating that the region became increasingly arid during the early to mid-Holocene with generally more moist conditions developing in the late Holocene. Some intriguing discrepancies are evident, however. In particular, the timing of both the onset and conclusion of this dry interval in LTCK appears to lag by one to several millennia behind Lake Titicaca, according to the oxygen isotope record. For instance, the water level at Lake Titicaca may have been 100 m lower than present as early as 10 200 cal yr BP (Cross et al., 2000), yet cellulose-inferred lake water oxygen isotope values at LTCK between 10 000 and 6200 cal yr BP are in the range of lakes that today are glacier-fed and overflowing. Diatom taxa in the LTCK core, however, become dominated by shallow water periphytic forms after 8500 cal yr BP consistent with changes in the physical sedimentology (Abbott et al., 1997b,

[3] All ages in this manuscript are reported as calibrated years (cal yr BP) according to INTCAL98 (Stuiver et al., 1998).

2000). The late Holocene shift to more moist conditions also appeared to be out-of-phase. At Lake Titicaca this developed at about 3500 cal yr BP (Abbott et al., 1997a), while this did not occur until after 2300 cal yr BP at LTCK (Abbott et al., 2000). Thus key questions remain regarding the spatial and temporal variability of early to mid-Holocene aridity in this region.

To evaluate the regional significance of the LTCK lake water oxygen isotope record, we examined the sediment record from Lago Potosi (LP), a seasonally closed lake in a watershed that is not presently glaciated, which should provide a more sensitive record of climate change (Fig. 1). Here we reconstruct the lake water oxygen isotope history for this site from sediment cellulose and compare it to our previous results from LTCK (Abbott et al., 2000). This comparison, in addition to other supporting isotopic and paleoclimatic evidence, provides the foundation for a preliminary quantitative reconstruction of summer relative humidity variation for the past 11 500 cal yr.

2. Climatic and hydrological setting

Precipitation in the Altiplano region is strongly seasonal with about 75% of the annual total occurring during the austral summer months (December to March) due to convective activity associated with the Bolivian High. Above average precipitation has been linked with strengthening and southward displacement of the Bolivian High while below average precipitation is associated with weakening and northward displacement (Aceituno and Montecinos, 1993). Latitudinal gradients in precipitation and relative humidity are evident between LTCK and LP. At El Alto, La Paz (4105 m above sea level (masl); 16°30′S; 68°12′W) in the northern Altiplano near LTCK, mean annual precipitation is 564 mm (December to March: 388 mm) and mean annual relative humidity is 60% (December to March: 70%) (Johnson, 1976). Further south at the town of Potosi (4640 masl; 19°38′S; 65°41′W) near LP, mean annual precipitation is 301.5 mm (December to March: 226 mm) and mean annual relative humidity is 38% (December to March: 50%) (Boletin Meteorologico Del Departmento De Potosi, 1996).

LTCK and LP have significantly different hydrological settings. The LTCK watershed (84 km^2) is located at 16°13′S, 68°21′W in the Rio Palcoco Valley on the western slope of the Cordillera Réal. Situated at 4300 masl in elevation, LTCK is 1.3 km^2 in area and 12 m deep.

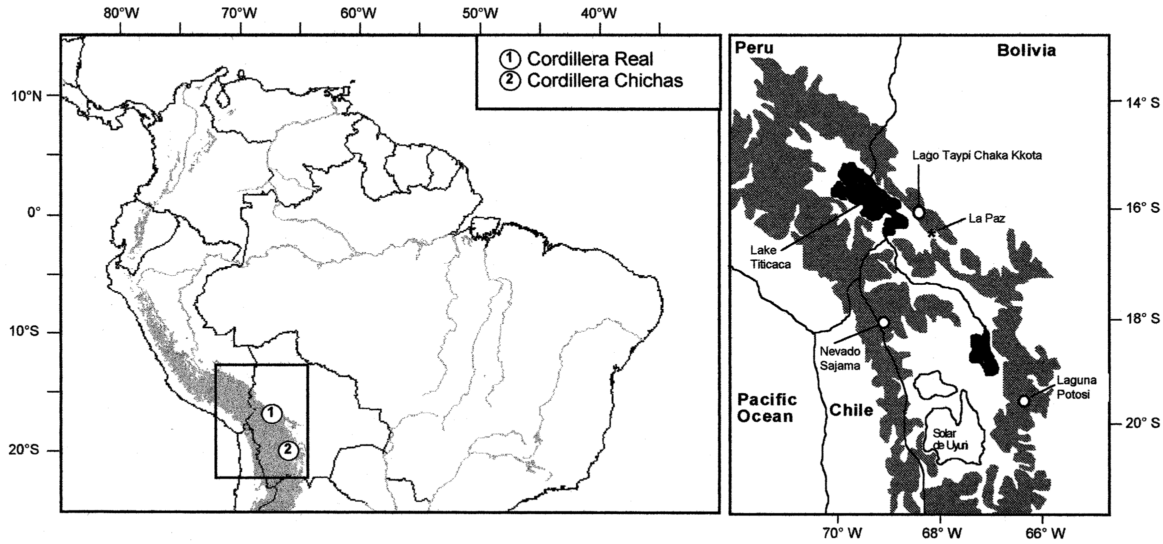

Fig. 1. Location map of study area. Shaded area represents elevations greater than 3000 m.

Through-flow at LTCK is maintained throughout the year by drainage from lakes upstream, which are presently fed by several small alpine glaciers. The LP watershed (3.9 km^2) is located at 19°38′S, 65°41′W in the Cordillera Chichas at 4640 masl and the lake is 0.2 km^2 in area and 11 m deep. LP is a headwater lake whose watershed does not presently contain glaciers. Cores and water samples were collected between June 12 and 16, 1997. LP formed a thin ice cover at night during this period and the lake was below its overflow level, although outflow channels suggest the water level reaches the overflowing stage during the summer wet season.

A regional water sampling survey spanning latitudes 13°54′ to 19°38′S, also conducted during the dry season of 1997, revealed that the $\delta^{18}O$ and δD composition of lake waters diverge from the Global Meteoric Water Line (GMWL) due to evaporative enrichment (Fig. 2; Abbott et al., 2000). A Regional Evaporation Line (REL) can be drawn through these data points ($\delta D = 5.1\delta^{18}O - 35.5$; $R^2 = 0.97$) indicating a common atmospheric moisture source for this region. Furthermore, the extent of evaporative enrichment for a given lake was found to vary systematically in relation to the local hydrological setting. Progressively increasing offset from the GMWL was found for lakes directly receiving glacial meltwater, overflowing lakes in glaciated watersheds, overflowing lakes in non-glaciated watersheds, and seasonally closed lakes. End-members of the hydrological spectrum in this region are well represented by the depleted isotopic composition of LTCK ($\delta^{18}O = -14.8$‰, $\delta D = -112$‰), typical for lakes in glaciated watersheds, and the comparatively enriched isotopic composition of LP ($\delta^{18}O = -5.6$‰, $\delta D = -59$‰), representing the group of lakes that develop hydrological closure during the dry season (Fig. 2).

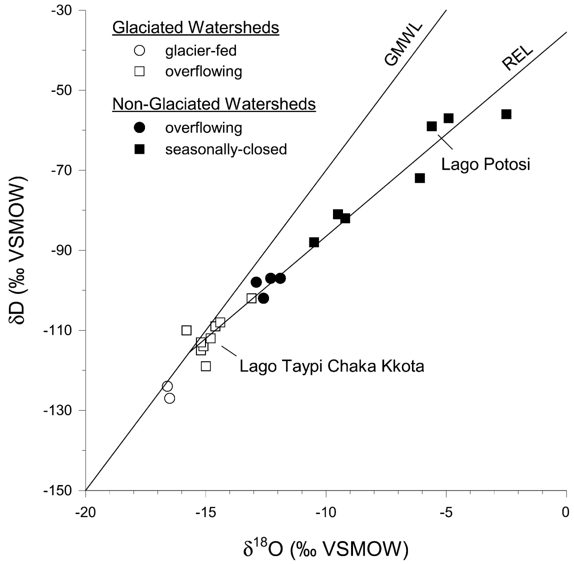

Fig. 2. Isotopic composition of lake waters from the Bolivian Andes sampled in June 1997 (from Abbott et al., 2000). Also shown are the GMWL ($\delta D = 8\ \delta^{18}O + 10$) and the REL ($\delta D = 5.1\ \delta^{18}O - 35.5$).

3. Materials and methods

Cores were taken from the center of LP at a water depth of 11 m using a square-rod piston corer (Wright et al., 1984) and a piston corer designed to collect the sediment–water interface (Fisher et al., 1992). Sample preparation and analysis for bulk organic elemental (C, N) and cellulose oxygen isotope composition followed methods in Wolfe et al. (2001). Briefly, samples were treated with 1 N HCl to remove carbonate material, rinsed repeatedly with distilled water, freeze-dried, and then passed through a 500-mm sieve to remove coarse debris. Carbon and nitrogen content were determined on the fine-grained acid-washed residue by an elemental analyzer interfaced to a continuous flow isotope ratio mass spectrometer. Additional sample treatment to concentrate cellulose involved solvent extraction, bleaching and alkaline hydrolysis to remove non-cellulose organic constituents plus leaching to remove iron and manganese oxyhydroxides. Cellulose oxygen isotope composition was determined using off-line nickel-tube pyrolysis to generate CO_2 for dual inlet isotope ratio mass spectrometry (Edwards et al., 1994). All elemental and isotopic analyses were conducted at the University of Waterloo Environmental Isotope Laboratory, Canada. Oxygen isotope results are expressed as 'δ' values, representing deviations in per mil (‰)

from the VSMOW standard for oxygen normalized to $\delta^{18}O_{SLAP} = -55.5‰$ (Coplen, 1996), such that $\delta_{sample} = [(R_{sample}/R_{standard}) - 1] \times 10^3$ where R is the $^{18}O/^{16}O$ ratio in the sample and standard. The LP $\delta^{18}O_{cell}$ values have uncertainties of $\pm 0.5‰$ (similar to the LTCK $\delta^{18}O_{cell}$ results; Abbott et al., 2000) based on repeated analyses of samples.

Terrestrial macrofossil material was not present in sufficient quantities for accelerator mass spectrometry (AMS) ^{14}C measurements from most stratigraphic levels. Therefore, we used *Isoetes* macrofossils at LTCK as well as bulk sediment at LP for AMS ^{14}C measurements. The contemporary radiocarbon reservoir was assessed in two ways. In LTCK, the ^{14}C activity of live submerged macrophytes was measured and found to be 114% Modern for the year A.D. 1992, indicating that the lake reservoir effect is minimal in the LTCK system today, although it could have been a factor in the past. In LP, the contemporary radiocarbon reservoir was assessed by comparing the ^{14}C activity of paired bulk sediment and macrofossil samples from the same stratigraphic level. Results indicate there is no significant difference between the ages.

4. Results and discussion

4.1. Lake sediment cellulose origin and surface-sediment–lake water relations

Constraints on the reconstruction of lake water $\delta^{18}O$ from cellulose $\delta^{18}O$ may be derived by considering the source of the organic matter, oxygen isotope fractionation between aquatic cellulose and water, and comparison between measured surface-sediment cellulose $\delta^{18}O$ and single-visit sampling and measurement of lake water $\delta^{18}O$. Previous work at LTCK showed that low C/N ratios measured on submerged aquatic vegetation in the lake (11.4 ± 3.6) and throughout the sediment core (ranging from 6.3 to 12.9) provided support for assuming a primarily aquatic origin in stratigraphic interpretation of the varying sediment cellulose isotopic composition (Abbott et al., 2000; see Table 1). Furthermore, $\delta^{18}O$ analyses of lake water, cellulose derived from aquatic plants, and surface-sediment cellulose were consistent with a cellulose–water oxygen isotope fractionation factor of 1.028 ± 0.001 (Abbott et al., 2000), which has been applied in most other settings and is based on both laboratory and field data (Sternberg, 1989; Yakir, 1992; Wolfe et al., 2001).

New C/N ratio data from LP, which are characterized by low values (<13.8 and mainly between 9 and 12), also suggest a dominantly aquatic origin for the fine-grained bulk organic matter for this site (Table 1). Additional hydrological information for LP may be extracted from the relationship between the surface-sediment cellulose-inferred $\delta^{18}O_{lw}$ ($-11.1 \pm 1.0‰$), based on a cellulose–water fractionation factor of 1.028 ± 0.001, and the measured $\delta^{18}O_{lw}$ ($-5.6‰$) (Table 1). This isotopic difference can most likely be attributed to the often unavoidable mismatch between single-episode lake water sampling of isotopic composition, which may be a reflection of conditions that took weeks to months to develop and the surface-sediment that integrates years to potentially decades or longer. Similar observations have been made at other lakes susceptible to strong seasonal isotopic variation. For example, single-episode water and surface-sediment sampling of small lakes in northern Russia during the early ice-free season showed that hydrological conditions inferred from the surface-sediments at most sites were systematically offset from those prevailing at the time of sampling due to the remnant influence of snowmelt on lake water isotopic composition (see Wolfe and Edwards, 1997). Additionally, lakes in northern Canada have been observed to vary seasonally by more than 5‰ in $\delta^{18}O$ under more moist conditions (Gibson et al., 1993, 1996).

At LP, lake water sampling was conducted during the dry season and thus, the sampled lake water at LP can be expected to be biased towards more enriched isotopic values that develop due to seasonal lake water evaporation and non-steady-state enrichment resulting from lake volume draw-down below the overflow level (Fig. 3). We speculate that substantial seasonal variability in lake water isotopic composition characterizes

Table 1
Bulk organic carbon/nitrogen weight ratios and cellulose-inferred $\delta^{18}O_{lw}$ values (including replicates) for LTCK and LP calculated using a cellulose–water fractionation factor of 1.028

Lago Taypi Chaka Kkota (measured $\delta^{18}O_{lw}$ in June 1997: −14.8‰)			Lago Potosi (measured $\delta^{18}O_{lw}$ in June 1997: −5.6‰)		
Core depth (cm)	C/N wt. ratios	cell-inf. $\delta^{18}O_{lw}$ (‰ VSMOW)	core depth (cm)	C/N wt. ratios	cell-inf. $\delta^{18}O_{lw}$ (‰ VSMOW)
0.0	7.6	−14.3	0.0	10.8	−11.1
5.5	7.6	−13.8	12.5	10.8	−9.6
11.5	8.5	−14.8 −15.2	22.5	11.6 11.5	−9.0
15.5	8.0	−16.5	36.5	10.5	−7.6
21.5	8.2	−13.2	48.5	10.0	−12.8
30.5	8.2	−12.6	60.5	9.4	−13.6
33.5	8.4	−9.6 −9.8	73.5	9.6	−14.5
39.5	8.0	−13.1	87.0	9.1 9.1	−7.6 −7.4
45.5	8.3	−13.8	100.0	10.3 10.3	−13.9 −12.5
48.5	8.3	−10.1	113.0	9.2	−7.0
50.5	7.2	−7.3	119.0	10.8	−3.5 −3.7
53.5	7.1	−9.1	130.0	9.2	−9.4
57.5	6.7 6.8	−9.5	139.0	10.1	−12.0 −10.7
60.5	6.7	−14.2 −13.0	150.0	10.1	−5.6
65.5	6.4	−6.9	164.0	10.3 10.2	−9.3 −10.5
70.5	7.6	−4.9 −5.6	173.5	10.3	−5.0
75.5	7.8 7.6	−6.9	183.5	10.1 10.2	−12.1 −12.2
80.5	10.1	−9.2	193.5	9.9	−8.3
85.5	10.1	−8.4	203.5	10.0	−6.0
90.5	11.7	−8.4	213.5	10.1	−7.6
94.5	10.7	−7.3	223.5	10.4 10.5	−10.6 −10.5
97.5	11.9	−7.1	233.5	10.4 10.4	−10.8 −10.2
99.5	11.8	−12.9	243.5	10.4	−10.8
112.0	11.2 11.0	−14.9 −14.2	253.5	10.0	−11.2 −11.8
120.5	12.1	−17.5 −16.1	271.0	9.8 9.8	−2.1 −2.8
128.5	10.5 10.1	−13.2	281.0	10.1	−3.7
138.0	12.9	−14.9	290.0	10.7	−7.2
142.0	11.6	−15.2	300.0	10.3	−5.3
147.5	12.0	−11.0	310.0	10.2 10.3	−3.7
153.5	10.7	−13.3	321.0	10.3	−6.4
165.0	12.3	−11.0	343.5	9.1 8.9	−13.2
175.0	11.4	−13.6	353.5	11.3	−12.5
176.0	11.7	−14.0	363.5	10.3	−11.0
184.0	11.0	−14.5	373.5	10.2	−6.9 −9.3
185.0	11.3	−13.2	383.5	11.7	−7.1 −7.4
193.0	10.2	−12.5	393.5	9.6	−13.3
199.0	9.9 9.2	−12.0	403.5	9.2	−11.7
205.0	11.0	−12.4	412.5	10.6	−16.6 −15.9
215.0	10.2	−11.3	423.5	11.5	−10.6
228.0	10.4	−13.9	435.5	11.4	−12.2
238.0	9.3	−8.8	445.5	11.2	−10.7
247.0	9.5	−8.2 −9.9	455.5	12.1	−13.5
262.0	9.2	−12.2	465.5	11.5	−12.9
276.0	8.5	−11.1	475.5	11.9	−14.6
288.0	6.3	−14.7	485.5	13.0 12.9	−10.2
			495.5	10.4 10.0	−16.2 −14.8
			538.0	13.8	−2.7 −4.0
			554.0	12.7	−13.2 −12.3
			604.5	13.8	−6.5 −7.8

Table 1 (*continued*)

Lago Taypi Chaka Kkota (measured $\delta^{18}O_{lw}$ in June 1997: −14.8‰)			Lago Potosi (measured $\delta^{18}O_{lw}$ in June 1997: −5.6‰)		
Core depth (cm)	C/N wt. ratios	cell-inf. $\delta^{18}O_{lw}$ (‰ VSMOW)	core depth (cm)	C/N wt. ratios	cell-inf. $\delta^{18}O_{lw}$ (‰ VSMOW)
			616.5	12.0	−11.0
			628.5	7.1	−12.7
			646.5	8.2 8.2	−10.0
			706.5	2.9	−11.2

LP, given its small volume, shifting water balance, combined with the low relative humidity in this region during the dry season (≈25%), although multiple water samples are obviously necessary to verify this hypothesis. Combined with the observation of episodic ice cover during the austral winter, which would inhibit aquatic plant growth during this season, suggests that the oxygen isotope composition of sediment cellulose at LP may mainly reflect average wet (summer) season oxygen isotope composition. In contrast, the larger volume of LTCK and perennially through-flow hydrological status likely leads to subdued seasonal isotopic variation at this site. These are conditions that would necessarily foster a good oxygen isotope match between the one-time water sampling event and that inferred from living aquatic plants and surface-sediment (Fig. 3).

4.2. Isotope-inferred lake paleohydrology

Overall, the cellulose-inferred $\delta^{18}O_{lw}$ record for LP ranges from −16.2 to −2.5‰ (Fig. 4), encompassing the complete range of isotopic values sampled in our regional survey of lake basins (Fig. 2). Longer-term trends, as inferred from three-point running means drawn through the raw data (representing roughly 500 years), indicate that $\delta^{18}O_{lw}$ values similar to present occur at the base of the record and are followed by a trend to higher values between 14 000 and 11 500 cal yr BP, although large fluctuations are evident in the raw data. Generally low $\delta^{18}O_{lw}$ values dominate between 11 500 and 9000 cal yr BP. This is followed by a step-wise interval of generally increasing $\delta^{18}O_{lw}$ values, culminating in maximum lake water ^{18}O-enrichment at about 6000 cal yr BP. Lake waters remain moderately enriched in ^{18}O until 2000 cal yr BP, although the raw data indicate substantially greater variability during this interval compared to most of the profile. At about 2000 cal yr BP, $\delta^{18}O_{lw}$ values decrease and then increase once again after 1000 cal yr BP.

Comparison of the LP $\delta^{18}O_{lw}$ profile with the smoothed three-point running mean $\delta^{18}O_{lw}$ record from LTCK show some differences due to the contrasting hydrological settings of these two lakes. The LTCK record shows increasing $\delta^{18}O_{lw}$ values between 14 000 and 10 500 cal yr, followed by a shift to lower values. This shift persists to 6000 cal yr BP in contrast to the LP $\delta^{18}O_{lw}$ record. Rapid ^{18}O-enrichment occurs at 6000 cal yr BP and is largely maintained until 2000 cal yr BP BP, although a weak trend to lower values is evident during this interval. After 2000 cal yr BP, $\delta^{18}O_{lw}$ values are generally low (Fig. 4). Notably, the overall higher variability in the raw $\delta^{18}O_{lw}$ data from LP is most likely attributed to the greater hydrological variability of this small, headwater lake (see Fig. 3; cf. Wolfe et al., 2000).

Interpretation of $\delta^{18}O_{lw}$ records requires identifying signals related to changes in the isotopic composition of source water, reflecting the integrated signature of surface and subsurface inflow and precipitation, from changing hydrological factors (often primarily evaporative enrichment) that may subsequently modify the isotopic content of the lake water. Deconvolution of these isotopic signals in lake sediments from this region benefit from an independent 25 000-year record of precipitation $\delta^{18}O$ ($\delta^{18}O_p$) from the Sajama ice core (Thompson et al., 1998; Fig. 1). The ice-core oxygen isotope stratigraphy, which is also shown in Fig. 4 as 100-year averages, illustrates that values at the base of this interval increased to

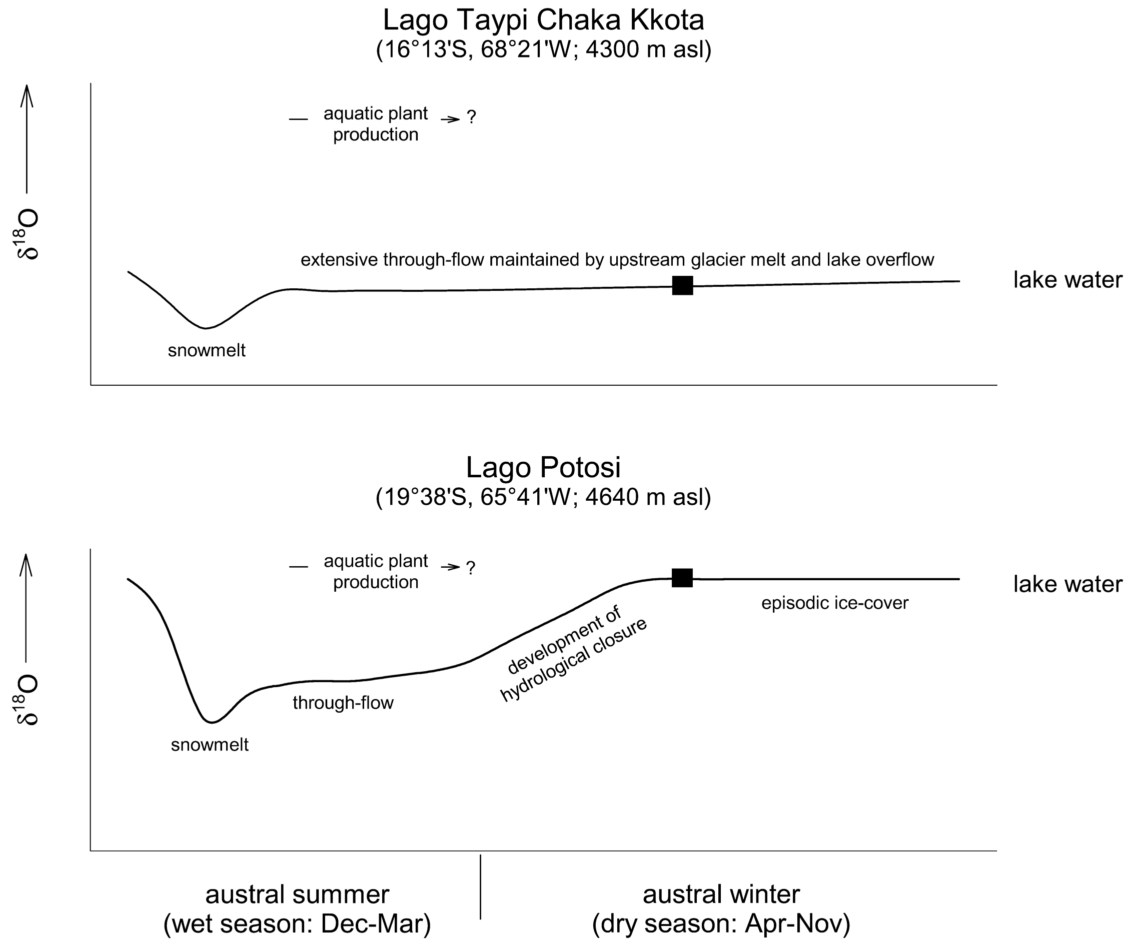

Fig. 3. Conceptual model of annual variation in lake water $\delta^{18}O$ ($\delta^{18}O_{lw}$) for LTCK and LP characterized by influx of ^{18}O-depleted runoff during snowmelt followed by enrichment due to evaporation. Perennially through-flow conditions at the former results in subdued seasonal variability in $\delta^{18}O_{lw}$ composition. Thus, the one-time water sampling event in June 1997 (represented by the solid square) provides a reasonable measure of average $\delta^{18}O_{lw}$ composition and which closely corresponds to values inferred from cellulose derived from aquatic plants sampled from the lake and the surface-sediment. In contrast, our one-time water sample from LP does not represent average $\delta^{18}O_{lw}$ composition due to marked seasonal variability. This stems from overflowing conditions during the austral summer, which is best represented by the surface-sediment cellulose, and hydrological closure with episodic ice-cover during the austral winter.

a maximum at about 14 300 cal yr BP, interpreted to reflect climate warming (Thompson et al., 1998). Subsequent ^{18}O-depletion with low values persisting until 11 500 cal yr BP has been interpreted as a climatic reversal (Thompson et al., 1998) or may be due to dilution of atmospheric precipitation with ^{18}O-depleted vapor derived from pluvial lakes on the Altiplano (Abbott et al., 2000). Values increase after 11 500 cal yr BP in response to climate warming (Thompson et al., 1998) and/or draw-down of pluvial lakes and reduction in derived vapor (Abbott et al., 2000) and remain at about -17 ± 1‰ throughout the Holocene. Notably, shifting LP and LTCK $\delta^{18}O_{lw}$ offsets from the Sajama ice core $\delta^{18}O_p$ record provides a measure of changing lake water evaporative enrichment (e.g. Seltzer et al., 2000), which appears to be mainly a function of similarly changing moisture regimes at these two locations, as described below.

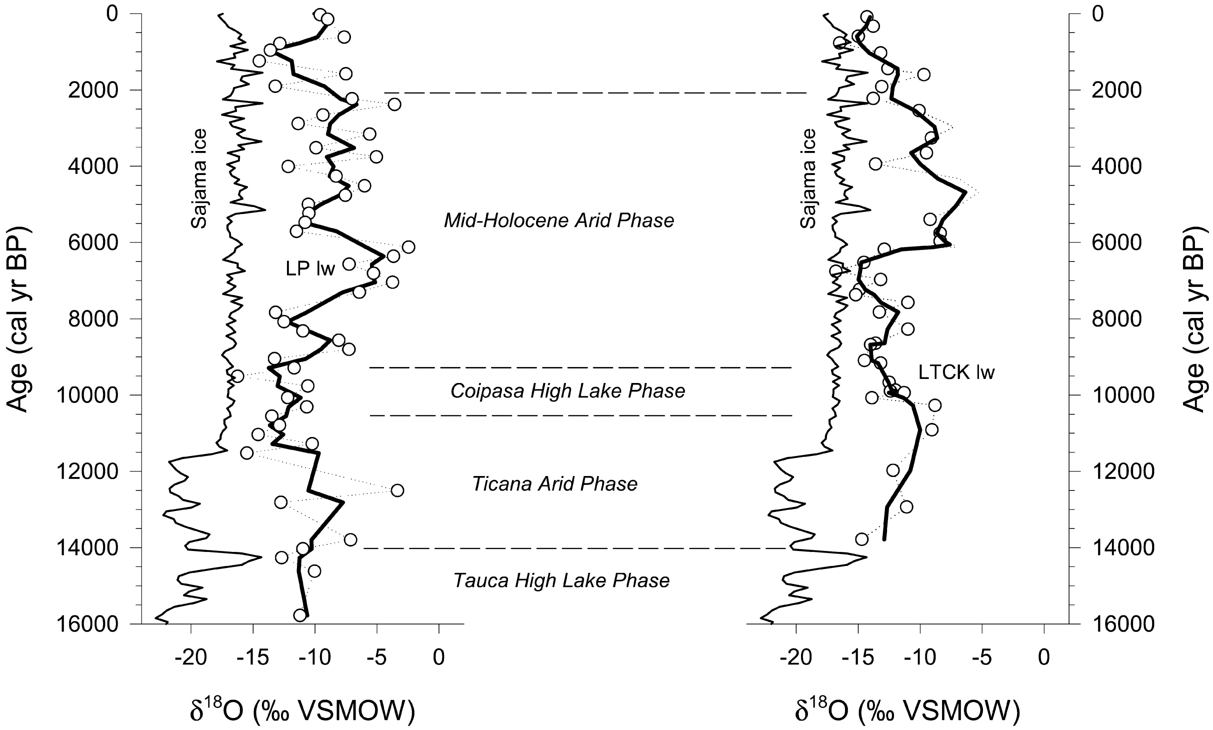

Fig. 4. Cellulose-inferred $\delta^{18}O_{lw}$ records for LP and LTCK versus cal yr BP (see Table 2). Solid lines represent three-point running means. Also shown is 16 000 cal yr of the $\delta^{18}O$ record in the Sajama ice core plotted as 100-year averages (Thompson et al., 1998), and stratigraphic zonation of major hydroclimatic intervals based partly on Sylvestre et al. (1999).

Although late Pleistocene $\delta^{18}O_{lw}$ data at both LP and LTCK are sparse, results are broadly consistent with regional evidence for moisture fluctuations derived from the recently revised chronology of pluvial lake level history on the southern Bolivian Altiplano (Sylvestre et al., 1999). Roughly 10‰ offset of LP $\delta^{18}O_{lw}$ from Sajama ice core $\delta^{18}O_p$ between 14 000 and 11 500 cal yr BP may reflect the importance of lake water evaporative enrichment, corresponding to the Ticaña arid phase (Sylvestre et al., 1999), or may be partly in response to reduced glacial

Table 2
Radiocarbon ages from LP measured at the Center for AMS (CAMS), Lawrence Livermore National Laboratory, and calibrated ages according to the methods outlined for INTCAL98 by Stuiver et al. (1998)

Depth (cm)	Material	Measured ^{14}C age (^{14}C yr BP)	$\delta^{13}C$ (‰ PDB)	Median calibrated ^{14}C age (cal yr BP)
31.5	aquatic macrofossil	560 ± 25	−13.0	545
59–61	aquatic macrofossil	1060 ± 40	−17.6	950
72–73	aquatic macrofossil	1270 ± 50	−17.5	1220
131.5	bulk (humic acid)	2460 ± 45	−19.8	2695
212.5	bulk (humic acid)	4220 ± 50	−19.5	4740
344.5	bulk (humic acid)	7050 ± 190	−19.0	7860
445.5	bulk (humic acid)	9350 ± 100	−21.1	10 310
527.5	aquatic macrofossil	$10\,400 \pm 95$	−23.7	12 300
632.5	> 125 μm	$12\,280 \pm 60$	−18.0	14 340

Radiocarbon data for LTCK have been reported previously (Abbott et al., 1997b, 2000).

meltwater supply. Reduced LP-Sajama isotopic offset after 11 500 until 9000 cal yr BP correlates with the final, albeit less significant, pluvial lake high stand (the Coipasa high lake phase), which occurred between about 10 500 and 9500 cal yr BP (Sylvestre et al., 1999). Similarly, large LTCK-Sajama isotopic offset beginning prior to 12 700 to about 10 500 cal yr BP may be related to the Ticaña arid phase with subsequent reduced isotopic offset until about 9500 cal yr BP due to wetter conditions during the Coipasa event. The lake water shift to more ^{18}O-depleted values, which we presume to indicate the end of the Ticaña arid phase, appears to take place about 1000 years later at LTCK compared to LP perhaps reflecting poor chronological control in these strata, a greater hydrological threshold at LTCK, or reduced significance of this climate change in the northern Bolivian Altiplano. The latter appears to be consistent with the greater prominence of this event in stratigraphic records from the southern Bolivian Altiplano and Chilean Atacama, whereas evidence for this event in Lake Titicaca sediment records is inconclusive (see Sylvestre et al., 1999).

Increasing aridity during the early Holocene at LP is indicated by lake water ^{18}O-enrichment beginning after 9000 cal yr BP, broadly consistent with the paleohydrological record of Lake Titicaca, although a brief return to moist conditions is suggested by ^{18}O-depleted values at about 8000 cal yr BP. Based on the LP record, maximum mid-Holocene aridity developed between 7500 and 6000 cal yr BP. The corresponding 9000 to 6000 cal yr BP interval at LTCK, which is dominated by ^{18}O-depleted values, is most likely a result of a local catchment effect, such as input of ^{18}O-depleted water from snowmelt or groundwater and rapid hydrological flushing (Abbott et al., 2000). Furthermore, abrupt ^{18}O-enrichment at 6000 cal yr BP observed in the LTCK record would appear to be consistent with a rapid change in water balance resulting from cessation of significant snowmelt and/or groundwater supply from the large catchment (Abbott et al., 2000) and very dry conditions.

Analysis of closely spaced samples has revealed substantial hydrological variability in the 6000 to 2000 cal yr BP $\delta^{18}O_{lw}$ record from LP. Highly variable oxygen isotope values have also been obtained on ostracode profiles in lake sediment cores from the Chilean Altiplano during this time interval suggesting predominantly arid conditions were punctuated by short-term climatic shifts (Schwalb et al., 1999). The transition to a more moist climate during the mid- to late Holocene was evidently a step-wise shift characterized by fluctuating moisture conditions on both the Bolivian and Chilean Altiplano (Valero-Garcés et al., 1996; Grosjean et al., 1997; Schwalb et al., 1999). Less variability observed in the LTCK $\delta^{18}O_{lw}$ during this interval is consistent with this lake's larger size and catchment, and the weak trend to lower $\delta^{18}O_{lw}$ values also suggests a gradual shift to more moist conditions overall.

The end of the mid-Holocene arid phase at LP is marked by a decline in $\delta^{18}O_{lw}$ values around 2000 cal yr BP, similar to the $\delta^{18}O_{lw}$ record from LTCK where glacial meltwater influx returned as a source for the lake (Abbott et al., 2000). This correlation lends support for a regional 1000–1500 year difference in the predominant shift to more moist conditions in the late Holocene compared to the Lake Titicaca record. A recent increase in aridity is suggested by ^{18}O-enrichment at both LTCK and LP after 1000 cal yr BP.

4.3. Quantitative reconstruction of paleohumidity

Largely coherent $\delta^{18}O_{lw}$ trends between LTCK and LP that conform to the regional paleoclimatic framework can be used to support a more quantitative description of changing paleohumidity by using an isotope-mass balance approach (Fig. 5a). At isotopic steady-state, the relationship between the fraction of lake water lost by evaporation and isotopic enrichment by evaporation for a lake with both inflow and outflow can be described by the following equations (Gat, 1981):

$$E/I = (1-h)/h \times (\delta_{lw}-\delta_p)/(\delta^*-\delta_{lw}) \qquad (1)$$

where E = vapor flux, I = inflow, h = relative humidity at the air–water interface (which may be

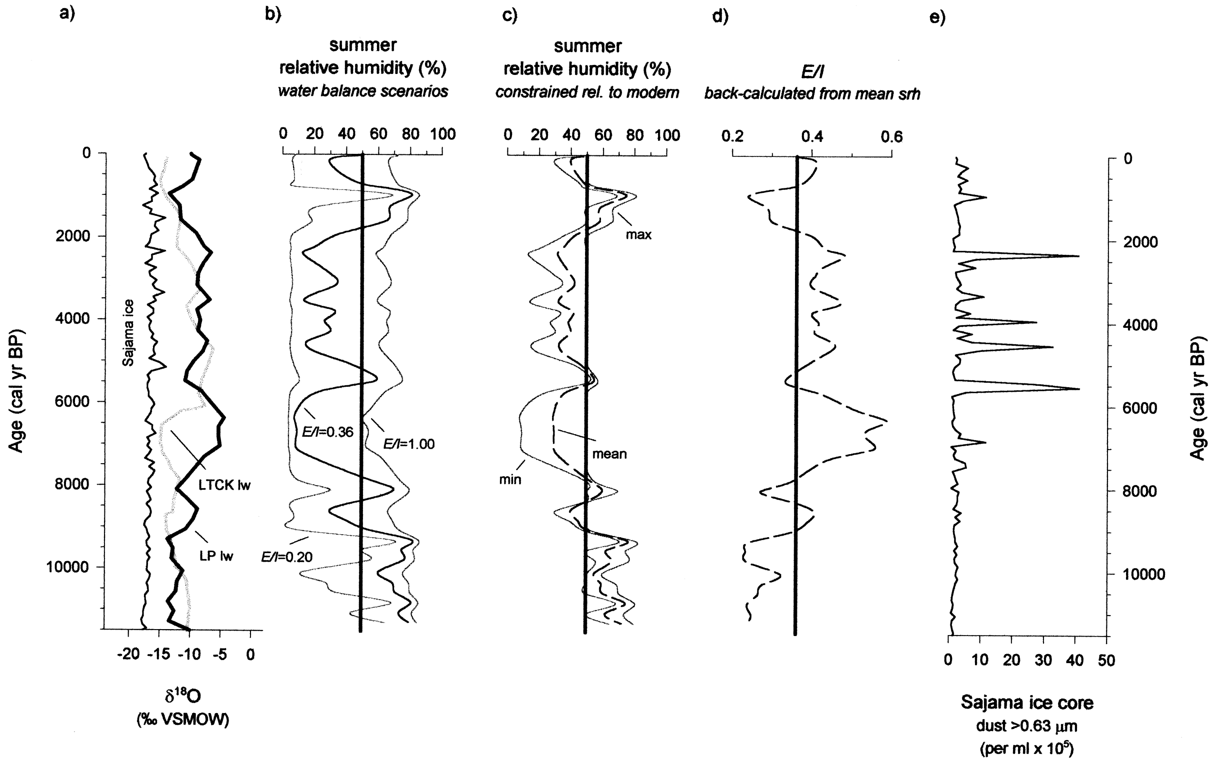

Fig. 5. (a) Sajama ice core $\delta^{18}O$ plotted as 100-year averages (Thompson et al., 1998) and cellulose-inferred three-point running mean $\delta^{18}O_{lw}$ records for LTCK and LP from Fig. 4. (b) Summer relative humidity profiles generated by *E*/*I* scenarios of 0.20, 0.36, and 1.00 based on the LP three-point running mean $\delta^{18}O_{lw}$ profile. (c) Summer relative humidity reconstruction representing minimum, maximum, and mean values constrained by values generated by the three *E*/*I* scenarios in (b) and the modern summer relative humidity value of 50%. (d) Estimated average summer water balance conditions (expressed as *E*/*I*) derived from back-calculation using mean summer relative humidity values in (c). (e) The Sajama ice core dust record from Thompson et al. (1998). All records are plotted versus cal yr BP.

slightly higher than ambient), δ^* = limiting isotopic enrichment attainable where the water body evaporates to near zero volume, δ_{lw} = lake water isotopic composition, δ_p = precipitation isotopic composition and

$$\delta^* = (h\delta_a + \varepsilon)/(h - \varepsilon) \tag{2}$$

where δ_a = vapor isotopic composition, ε = isotopic separation between liquid and vapor including both equilibrium (ε^*) and kinetic (ε_K) effects.

Isotope-mass balance methods can be used to assess contemporary water balance of lakes (e.g. Gat and Levy, 1978; Gibson et al., 1993), as well as to reconstruct past hydrology and climate from lacustrine records of $\delta^{18}O$ (e.g. Edwards et al., 1996; Wei and Gasse, 1999). Here, we use this model to estimate summer relative paleohumidity (SRH) from the LP cellulose-inferred three-point running mean $\delta^{18}O_{lw}$ record. The LP $\delta^{18}O_{lw}$ record was chosen for SRH reconstruction because the record at this site does not appear to be complicated by additional hydrological effects, as is the case at LTCK during the early Holocene (possible snowmelt and/or groundwater supply) and late Holocene (glacial meltwater influx; see Abbott et al., 2000). The reconstruction is limited to the past 11 500 cal yr where the LP $\delta^{18}O_{lw}$ record is more highly resolved and temporally constrained. Model input values include: (1) $\delta_p = -17$‰ estimated from the Sajama ice core 100-year average $\delta^{18}O$ record (Fig. 4), which also closely approximates the intersection of the REL and GMWL in Fig. 2[4], (2) $\delta_a = \delta_p - \varepsilon^*$ (i.e. isotopic equilibrium between atmospheric vapor and precipitation), (3) $\varepsilon^* = 10.66$‰ from Majoube (1971) and using an average air temperature of 10°C (Boletin Meteorologico Del Departmento De Potosi, 1996), and (4) $\varepsilon_K = 14.2(1-h)$ (Gonfiantini, 1986).

SRH is solved iteratively for three water balance scenarios that conservatively span the probable maximum range in natural variability over the past 11 500 cal yr (Fig. 5b). (1) $E/I = 1.00$ defines conditions for a terminal basin where evaporation balances inflow so that no liquid outflow occurs. This represents the maximum fraction of lake water lost by evaporation as long-term hydrological status characterized by $E/I > 1$ is considered unlikely because this would lead to lake desiccation and absence of a stratigraphic record. (2) $E/I = 0.20$ was used to represent the minimum fraction of lake water lost by evaporation. This value is estimated from calculation of modern E/I ratios for overflowing lakes in non-glaciated watersheds and using the most isotopically enriched lake water sample in our modern data set as a lower limit for δ^* (Fig. 2). (3) $E/I = 0.36$ represents an estimate of the average summer water balance at present for LP based on a modern SRH value of 50% (Boletin Meteorologico Del Departmento De Potosi, 1996). Comparison to modern conditions was used to derive a range in SRH values, bracketing concomitant water balance response to changing effective moisture using the three E/I scenarios. Results are plotted in Fig. 5c in terms of minimum, maximum and mean SRH values.

In general, results from Fig. 5c show that SRH values averaged 10–20% higher relative to present at 11 500 cal yr BP with oscillating but generally declining values developing during the early Holocene. This trend culminates in maximum SRH decrease between 7500 and 6000 cal yr BP when reconstructed values average 20% lower than present. SRH values are near present between 6000 and 5000 cal yr BP and then decline to values averaging 15% lower than present until about 2500 cal yr BP. Mean SRH values increase to about 20% greater than present by about 1500 cal yr BP and then decline to around 5–10% less than present over the last 1000 years.

Notably large ranges between minimum and maximum SRH values are evident at low SRH compared to the present value of 50%, which is primarily a function of the large uncertainty in E/I ratios (0.36 to close to 1.00) that bracket these intervals. This extreme sensitivity is somewhat artificial, however, because the actual E/I ratios are relatively high during phases of low SRH, although not as high as 1.00 as values generated by this scenario are nearly always higher than 50%. This indicates that LP may have rarely attained wet-season terminal hydrological status for an extended period even during more arid intervals; a result that is not unexpected, however, as overcoming this threshold would likely have led to rapid volume draw-down, lake desiccation and hiatuses in sedimentation due to the low relative humidity. Indeed, the $\delta^{18}O_{lw}$ record is very sensitive to SRH below about 50% and because extreme ^{18}O-enrichment is not observed, SRH values substantially less than 40% are probably not reasonable. Conversely, less uncertainty is evident at high SRH mainly because of the narrower range in E/I ratios (0.20–0.36) that were used to delineate these phases (mainly 11 500 to 9000 and 2000 to 1000 cal yr BP). Based on back-calculation using the mean SRH reconstruction, we estimate that the average summer E/I ratio spanned mainly from about 0.25 to 0.60 over the past 11 500 cal yr (Fig. 5d).

Although our SRH reconstruction is solely based on the LP $\delta^{18}O_{lw}$ record, supporting evidence for widespread and similarly arid conditions during the mid- to late Holocene is pro-

[4] Intersection of the REL with the GMWL provides a first-order estimate of the regional mean annual precipitation $\delta^{18}O$ (Gibson et al., 1993). As reported in Abbott et al. (2000), this value is −16‰. Note, however, that the lake water samples were taken during the dry season and are likely biased to more enriched values, which can influence the intersection of the REL and GMWL. Glacier-fed lakes in Fig. 2 that plot on the GMWL likely have suppressed seasonal variability and have $\delta^{18}O$ values of −16.6 and −16.5‰, close to the estimate from the Sajama ice core record. Uncertainty in $\delta^{18}O_p$ of ±1‰ is incorporated into a sensitivity analysis presented below.

vided by the LTCK $\delta^{18}O_{lw}$ profile and other records of past climate change. Between 6000 and 2000 cal yr BP, the $\delta^{18}O_{lw}$ values are broadly similar (Fig. 5a) and in the range of lakes that presently drop below their overflow level under more moderate conditions (Fig. 2). These overlapping trends may reflect similar *E*/*I* ratios and SRH during this time interval. Offset in cellulose-inferred $\delta^{18}O_{lw}$ over the last 1000 years suggests that the current effective moisture gradient between these two lakes may be a recent development. SRH minima during the mid- to late Holocene interval also shows close correspondence between dust concentration maxima in the Sajama ice core record, with both records reflecting dominantly arid but highly variable moisture conditions (Fig. 5e), in agreement with other records on the Chilean Altiplano as mentioned above (Valero-Garcés et al., 1996; Grosjean et al., 1997; Schwalb et al., 1999). Lake Titicaca lowstands at about 6100 and 2400 cal yr BP (Abbott et al., 1997a; Mourguiart et al., 1998) and lake-level-inferred maximum aridity between 8000 and 5500 cal yr BP (Baker et al., 2001) also compare well with the SRH reconstruction.

4.3.1. Model uncertainties

A sensitivity analysis was conducted to estimate potential sources of error associated with input parameters to Eqs. 1 and 2 to derive past SRH values, in addition to uncertainties due to shifting *E*/*I*. Fig. 6 illustrates the effect of $\delta_{lw} = \pm 1.5‰$, $\delta_p = \pm 1.0‰$, $T = \pm 5°C$, and $\delta_a = \delta_p - \pm 10\%(\varepsilon^*)$ on reconstructed SRH values for two water balance scenarios: (1) $E/I = 0.30$, which is estimated to reflect average conditions during wet intervals, and (2) $E/I = 0.50$ corresponding to estimated average conditions during dry phases (see Fig. 5d). Overall, potential error in SRH values is less in the $E/I = 0.50$ scenario, with δ_{lw} and δ_p input variations resulting in mostly $< 10\%$ error, and T and δ_a input variations producing $< 5\%$ error. Potential SRH errors are greater in the $E/I = 0.30$ scenario, although only $\delta_{lw} - 1.5‰$ and $\delta_p + 1‰$ variations over a narrow range of $\delta^{18}O_{lw}$ values result in errors in excess of (+)15%.

5. Conclusion

Comparison of cellulose-inferred lake water oxygen isotope profiles from two lakes in the Bolivian Andes provides a record of late Pleistocene and Holocene paleohydrological history that is largely in agreement with the regional framework based mainly on pluvial lake history, water level changes in Lake Titicaca, and the Sajama ice core record. Broad millennial-scale changes in Holocene effective moisture in the tropics have been linked to latitudinal migration of the Intertropical Convergence Zone driven by changes in insolation (Martin et al., 1997; Abbott et al., 1997b; Cross et al., 2000; Seltzer et al., 2000), although it should be noted that strikingly different effective moisture reconstructions have recently been reported in the Chilean Atacama by Betancourt et al. (2000). Additional differences between Bolivian Altiplano records continue to persist, such as the predominant shift in effective moisture during the late Holocene appears to lag by about 1000 to 2000 years in small, alpine lakes compared to Lake Titicaca, and further work is needed to explain this temporal discrepancy as well as the climate-driver for the high-frequency fluctuations.

Overall, the isotopic records indicate dominantly moist conditions during the late Pleistocene–early Holocene transition (roughly 10 500 to 9000 cal yr BP) and between 2000 and 1000 cal yr BP, whereas more arid conditions prevailed during the mid-late Holocene (mainly 8000 to 2000 cal yr BP) and over the past millennium. At LP, sustained maximum mid-Holocene aridity occurred between 7500 and 6000 cal yr BP and quantitative reconstruction of SRH, based on an isotope-mass balance model, indicates a decline of perhaps as much as 20% during this time. SRH values averaged 15% less than present but was highly variable during the later part of the mid-Holocene arid interval (ca. 5000–2000 cal yr BP), in agreement with other paleoclimatic records from the region (Valero-Garcés et al., 1996; Grosjean et al., 1997; Abbott et al., 1997a,b; Schwalb et al., 1999) including the Sajama ice core record where close correspondence occurs between several elevated dust particle concentrations (Thompson et al., 1998) and SRH minima. Sensitivity analyses suggests potential errors in re-

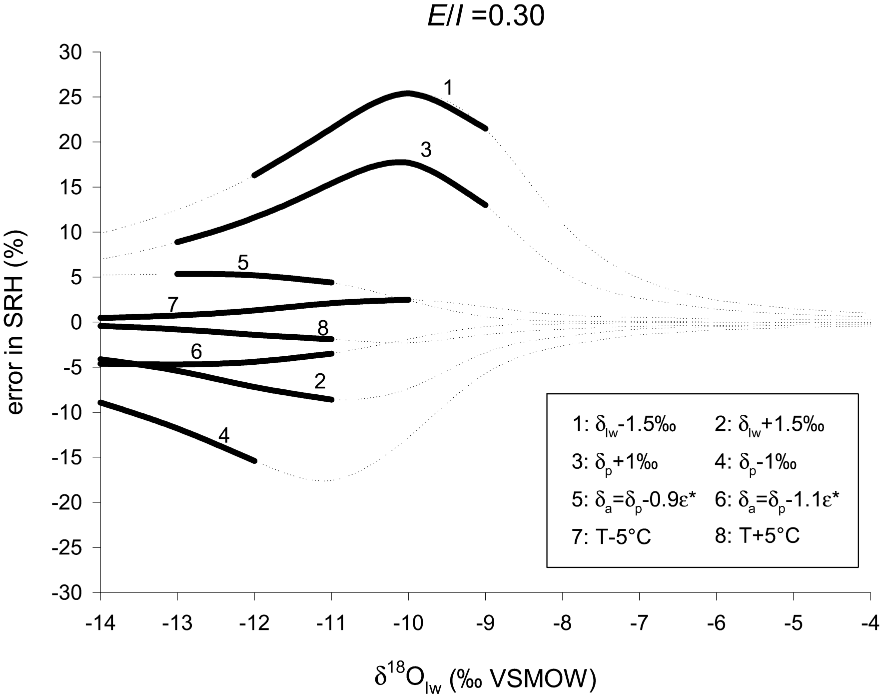
E/I =0.30
error in SRH (%)
δ18Olw (‰ VSMOW)
1: δlw-1.5‰
2: δlw+1.5‰
3: δp+1‰
4: δp-1‰
5: δa=δp-0.9ε*
6: δa=δp-1.1ε*
7: T-5°C
8: T+5°C

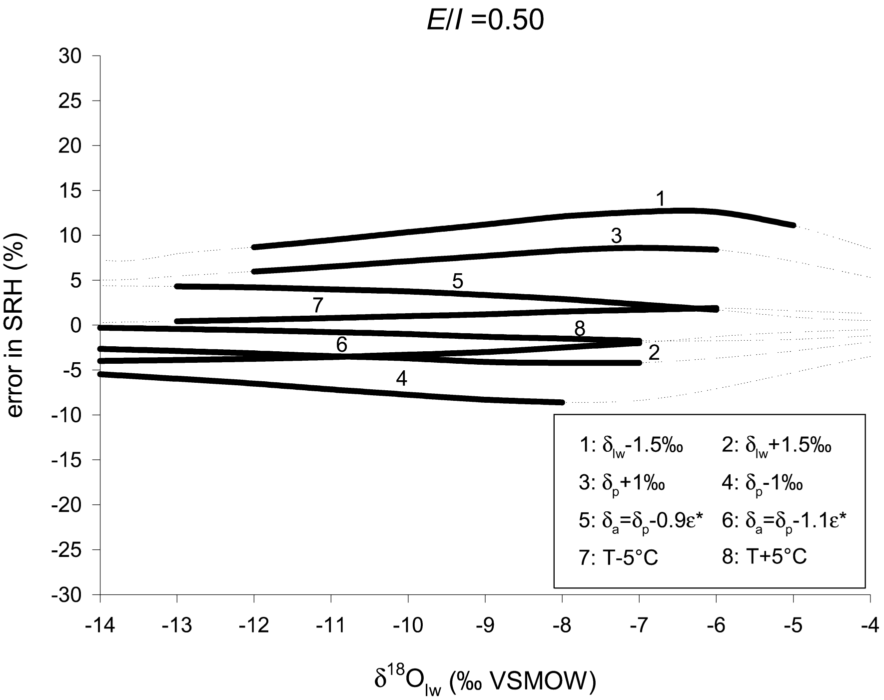
E/I =0.50
error in SRH (%)
δ18Olw (‰ VSMOW)
1: δlw-1.5‰
2: δlw+1.5‰
3: δp+1‰
4: δp-1‰
5: δa=δp-0.9ε*
6: δa=δp-1.1ε*
7: T-5°C
8: T+5°C

Fig. 6. Sensitivity analysis illustrating potential errors in summer relative humidity (SRH) values for variations of $\delta_{lw} = \pm 1.5‰$ (incorporating analytical and cellulose–water oxygen isotope fractionation uncertainty), $\delta_p = \pm 1.0‰$ (comprising most of the variation in the 100-year averaged isotopic record from Sajama ice core over the past 11 500 cal yr BP; Thompson et al., 1998), $T = \pm 5°C$ (estimated to reflect changes during the late Pleistocene–early Holocene transition and possibly during the interval of maximum aridity), and $\delta_a = \delta_p - \pm 10\%(\varepsilon^*)$(10% deviation from isotopic equilibrium between δ_a and δ_p). Results are shown for the average summer *E*/*I* ratio during wet (0.30) and dry intervals (0.50), as estimated from Fig. 5d. Note that solid lines define SRH errors that result in absolute values ranging from 30 to 85%, representing an estimate of the natural range potential in SRH.

constructed SRH values are mainly related to uncertainty in the *E*/*I* ratio during arid intervals and cellulose-inferred $\delta^{18}O_{lw}$ and ice-inferred $\delta^{18}O_p$ values during wet intervals.

Notably, the SRH reconstruction sets the stage for comparison with new proxy records currently being obtained from similar lakes north of the equator in the Venezuelan Andes (Abbott et al., 1999; Polissar et al., 2000). In addition, these results reveal the potential for quantitative paleoclimatic reconstructions based on cellulose-inferred lake water oxygen isotope records. Key factors that have contributed to the viability of this approach include an independent detailed record of $\delta^{18}O_p$ and analysis of lake sediment records in contrasting settings, the latter having effectively allowed differentiation of local hydrological variations from regional climatic changes.

Acknowledgements

Comments by A. Longinelli, an anonymous reviewer, and T. Edwards helped to clarify several aspects of the manuscript. We also thank L. Thompson for providing data from the Sajama ice core and A. Wolfe for assistance in obtaining the lake sediment cores. Assistance with sample preparation and analysis by R. Elgood and the UW-EIL is greatly appreciated. This research was funded by NSF Grant ATM-9632267 to M.B.A. and ATM-9613991 to G.O.S. Additional financial support was provided by an NSERC postdoctoral fellowship to B.B.W.

References

Abbott, M.B., Binford, M.W., Brenner, M., Kelts, K.R., 1997a. A 3500 ^{14}C yr high-resolution record of lake level changes in Lake Titicaca, Bolivia/Peru. Quat. Res. 47, 169–180.

Abbott, M.B., Seltzer, G.O., Kelts, K.R., Southon, J., 1997b. Holocene paleohydrology of the tropical Andes from lake records. Quat. Res. 47, 70–80.

Abbott, M.B., Wolfe, A.P., Polissar, P.J., Seltzer, G.O., Rodbell, D.T., 1999. Comparison of Holocene paleoclimate records from mountain lakes in the northern and southern hemispheres of tropical South America. American Geophysical Union Fall Meeting, U12A-16.

Abbott, M.B., Wolfe, B.B., Aravena, R., Wolfe, A.P., Seltzer, G.O., 2000. Holocene hydrological reconstructions from stable isotopes and palaeolimnology, Cordillera Real, Bolivia. Quat Sci. Rev. 19, 1801–1820.

Aceituno, P., Montecinos, A., 1993. Circulation anomalies associated with dry and wet periods in the South American Altiplano, Fourth International Conference on Southern Hemisphere Meteorology and Oceanography. American Meteorological Society, pp. 330–331.

Baker, P.A., Seltzer, G.O., Fritz, S.C., Dunbar, R.B., Grove, M.J., Tapia, P.M., Cross, S.L., Rowe, H.D., Broda, J.P., 2001. The history of South American tropical precipitation for the past 25 000 years. Science 291, 640–643.

Betancourt, J.L., Latorre, C., Rech, J.A., Quade, J., Rylander, K.A., 2000. A 22 000-year record of monsoonal precipitation from northern Chile's Atacama desert. Science 289, 1542–1546.

Binford, M.W., Kolata, A.L., Brenner, M., Janusek, J., Abbott, M.B., Curtis, J., 1997. Climate variation and the rise and fall of an Andean civilization. Quat. Res. 47, 171–186.

Boletin Meteorologico Del Departmento De Potosi, 1996. Servicio National De Meteorolgia E Hidrologia (SENAMHI). Potosi, Bolivia.

Clayton, J.D., Clapperton, C.M., 1997. Broad synchrony of a late-glacial glacier advance and the highstand of paleolake Tauca in the Bolivian Altiplano. J. Quat. Sci. 12, 169–182.

Coplen, T.B., 1996. New guidelines for reporting stable hydrogen, carbon, and oxygen isotope-ratio data. Geochim. Cosmochim. Acta 60, 3359–3360.

Cross, S.L., Baker, P.A., Seltzer, G.O., Fritz, S.C., Dunbar, R.B., 2000. A new estimate of the Holocene lowstand level of Lake Titicaca, central Andes, and implications for Tropical palaeohydrology. Holocene 10, 21–32.

Edwards, T.W.D., Buhay, W.M., Elgood, R.J., Jiang, H.B., 1994. An improved nickel-tube pyrolysis method for oxygen isotope analysis of organic matter and water. Chem. Geo. (Iso. Geosci. Sect.) 114, 179–183.

Edwards, T.W.D., Wolfe, B.B., MacDonald, G.M., 1996. Influence of changing atmospheric circulation on precipitation δ^{18}O-temperature relations in Canada during the Holocene. Quat. Res. 46, 211–218.

Fisher, M.M., Brenner, M., Reddy, K.R., 1992. A simple, inexpensive piston corer for collecting undisturbed sediment/water interface profiles. J. Paleolim. 7, 157–161.

Gat, J.R., 1981. Lakes. In: Gat, J.R., Gonfiantini, R. (Eds.), Stable Isotope Hydrology: Deuterium and Oxygen-18 in the Water Cycle. Technical Report Series No. 210, IAEA, Vienna, pp. 203–221.

Gat, J.R., Levy, Y., 1978. Isotope hydrology of inland sabkhas in the Bardawil area, Sinai. Limnol. Oceanogr. 23, 841–850.

Gibson, J.J., Edwards, T.W.D., Bursey, G.G., Prowse, T.D., 1993. Estimating evaporation using stable isotopes: quantitative results and sensitivity analysis for two catchments in northern Canada. Nord. Hydrol. 24, 79–94.

Gibson, J.J., Prowse, T.D., Edwards, T.W.D., 1996. Development and validation of an isotopic method for estimating lake evaporation. Hydrol. Process. 10, 1369–1382.

Gonfiantini, R., 1986. Environmental isotopes in lake studies. In: Fritz, P., Fontes, F.Ch. (Eds.), Handbook of Environmental Isotope Geochemistry, Vol. 2. Elsevier, New York, pp. 113–168.

Grosjean, M., Valero-Garcés, B., Geyh, M.A., Messerli, B., Schreier, H., Kelts, K., 1997. Mid and late Holocene limnogeology of Laguna del Negro Francisco (South-Central Andes, North Chile) and paleoclimatic implications. Holocene 7, 151–159.

Johnson, A.M., 1976. The climate of Peru, Bolivia, and Ecuador. In: Schwerdtfeger, W. (Ed.), Climates of Central and South America. Elsevier, Amsterdam, pp. 147–218.

Majoube, M., 1971. Fractionnement en oxygéne et en deutérium entre l'eau et sa vapeur. J. Chim. Phys. 197, 1423–1436.

Martin, L., Bertaux, J., Corrège, T., Ledru, M-P., Mourguiart, P., Suguio, K., Turcq, B., 1997. Astronomical forcing of contrasting rainfall changes in tropical South America between 12 400 and 8800 cal yr B.P.. Quat. Res. 47, 117–122.

Mourguiart, Ph., Corrège, T., Wirrmann, D., Argollo, J., Montenegro, M.E., Pourchet, M., Carbonel, P., 1998. Holocene palaeohydrology of Lake Titicaca estimated from an ostracod-based transfer function. Palaeogeogr. Palaeoclimatol. Palaeoecol. 143, 51–72.

Polissar, P.J., Abbott, M.B., Wolfe, A.P., Finney, B.P., Bradley, R.S., 2000. Holocene paleoclimatology of the Venezuelan Andes: preliminary results from Laguna Verdes Alta. American Geophysical Union Fall Meeting, OS11C-40.

Schwalb, A., Burns, S.J., Kelts, K., 1999. Holocene environments from stable isotope stratigraphy of ostracods and authigenic carbonate in Chilean Altiplano lakes. Palaeogeogr. Palaeoclimatol. Palaeoecol. 148, 153–168.

Seltzer, G.O., Baker, P., Cross, S., Dunbar, R., Fritz, S., 1998. High-resolution seismic reflection profiles from Lake Titicaca, Peru-Bolivia: evidence for Holocene aridity in the tropical Andes. Geology 26, 167–170.

Seltzer, G.O., Rodbell, D., Burns, S., 2000. Isotopic evidence for late Quaternary climatic change in tropical South America. Geology 28, 35–38.

Sternberg, L.S.L., 1989. Oxygen and hydrogen isotope ratios in plant cellulose: mechanisms and applications. In: Rundel, P.W., Ehleringer, J.R., Nagy, K.A. (Eds.), Stable Isotopes in Ecological Research. Springer, New York, pp. 124–141.

Stuiver, M., Reimer, P.J., Bard, E., Beck, J.W., Burr, G.S., Hughen, K.A., Kromer, B., McCormac, F.G., v.d. Plicht, J., Spurk, M., 1998. INTCAL98 Radiocarbon age calibration 24 000–0 cal BP. Radiocarbon 40, 1041–1083.

Sylvestre, F., Servant, M., Servant-Vildary, S., Causse, C., Fournier, M., Ybert, J.P., 1999. Lake-level chronology on the southern Bolivian Altiplano (18–23°S) during late-glacial time and the early Holocene. Quat. Res. 51, 54–66.

Thompson, L.G., Davis, M.E., Mosley-Thompson, E., Sowers, T.A., Henderson, K.A., Zagorodnov, V.S., Lin, P.-N., Mikhalenko, V.N., Campen, R.K., Bolzan, J.F., Cole-Dai, J., Francou, B., 1998. A 25 000-year tropical climate history from Bolivian ice cores. Science 282, 1858–1864.

Valero-Garcés, B.L., Grosjean, M., Schwalb, A., Geyh, M., Messerli, B., Kelts, K., 1996. Limnogeology of Laguna Miscanti: evidence for mid to late Holocene moisture changes in the Atacama Altiplano (northern Chile). J. Paleolim. 16, 1–21.

Wei, K., Gasse, F., 1999. Oxygen isotopes in lacustrine carbonates of West China revisited: implications for post glacial changes in summer monsoon circulation. Quat. Sci. Rev. 18, 1315–1334.

Wirrmann, D., de Oliviera Almeida, L.F., 1987. Low Holocene level (7700 to 3650 years ago) of Lake Titicaca (Bolivia). Palaeogeogr. Palaeoclimatol. Palaeoecol. 59, 315–323.

Wirrmann, D., Mourguiart, P., 1995. Late Quaternary spatio-temporal limnological variations in the Altiplano of Bolivia and Peru. Quat. Res. 43, 344–354.

Wolfe, B.B., Edwards, T.W.D., 1997. Hydrologic control on the oxygen-isotope relation between sediment cellulose and lake water, western Taimyr Peninsula, Russia: implications for the use of surface-sediment calibrations in paleolimnology. J. Paleolim. 18, 283–291.

Wolfe, B.B., Edwards, T.W.D., Aravena, R., Forman, S.L., Warner, B.G., Velichko, A.A., MacDonald, G.M.., 2000. Holocene paleohydrology and paleoclimate at treeline, north-central Russia, inferred from oxygen isotope records in lake sediment cellulose. Quat. Res. 53, 319–329.

Wolfe, B.B., Edwards, T.W.D., Beuning, K.R.M., Elgood, R.J., 2001. Carbon and oxygen isotope analysis of lake sediment cellulose: methods and applications. In: Last, W.M., Smol, J.P. (Eds.), Tracking Environmental Change using Lake Sediments, Vol. 2: Physical and Chemical Techniques. Kluwer Academic Publishers, Dordrecht, in press.

Wright, H.E., Mann, D.H., Glaser, P.H., 1984. Piston corers for peat and lake sediments. Ecology 65, 657–659.

Yakir, D., 1992. Variations in the natural abundance of oxygen-18 and deuterium in plant carbohydrates. Plant Cell Environ. 15, 1005–1020.